Investigation of the adsorption characteristics of Pb(II) onto natural kaolinite and bentonite clays

Gang Li[a], Xing Liu[a], Jinli Zhang[b,*], Jia Liu[c], Yiran Yang[a]

[a]*Shaanxi Key Laboratory of Safety and Durability of Concrete Structures, Xijing University, Xi'an, Shaanxi 710123, China,
Tel. +86-15991735077; email: T_bag945@126.com (G. Li), Tel. +86-18992299399; email: 2316541678@qq.com (X. Liu),
Tel. +86-18392589291; email: yryangxa@163.com (Y.R. Yang)*
[b]*State Key Laboratory of Coastal and Offshore Engineering, Dalian University of Technology, Dalian, Liaoning 116024, China,
Tel. +86-13940949667; email: jlzhang@dlut.edu.cn (J.L. Zhang)*
[c]*School of Geological Engineering and Geomatics, Chang'an University, Xi'an, Shaanxi 710054, China, Tel. +86-15929935077;
email: 15929935077@163.com (J. Liu)*

ABSTRACT

Pb(II) pollution threatens human health and environmental safety, and suitable adsorption materials are important for Pb(II) removal. In this study, the adsorption characteristics of Pb(II) onto natural kaolinite and bentonite in the Dalian and Heishan areas (China) were investigated, and the effects of the solid-to-liquid ratio, pH, temperature, and reaction time on the adsorption performance of Pb(II) were analyzed. The results showed that the adsorption capacity of kaolinite decreases as the solid-to-liquid ratio increases, whereas the adsorption capacity of bentonite first increases to a maximum and then decreases. The processes by which kaolinite and bentonite adsorb Pb(II) are both rapid, in which adsorption equilibrium is reached within 120 min, and the pseudo-second-order kinetic model provides the best fit to the experimental results. The Langmuir model provides the best simulation of the isothermal adsorption characteristics of Pb(II) onto kaolinite and bentonite. The adsorption of Pb(II) onto kaolinite is a spontaneous, exothermic, and entropy-decreasing process, where a lower temperature is beneficial for adsorption. However, the adsorption of Pb(II) onto bentonite is a spontaneous, endothermic, and entropy-increasing process, where high temperature is beneficial for adsorption. The results indicate that both natural kaolinite and bentonite can be used as effective adsorbents for Pb(II) removal.

Keywords: Adsorption; Pb(II); Kaolinite; Bentonite; Langmuir model

1. Introduction

The rising pollution of water resources, soil and air as a result of rapid industrialization, urbanization and economic development over the last several decades has led to grave global concern [1]. The liquid effluents mostly laden with heavy metals such as cadmium, cobalt, zinc, copper, or lead from several industries threaten the aquatic environment [2]. Due to their non-biodegradability and carcinogenicity, the pollution of aqueous streams by heavy metals is primarily worrisome [3]. When lead ions enter water and soil in large quantities, they agglomerate in the bodies of animals and plants through the food chain and cause serious environmental pollution, thus endangering human health [4,5]. According to regulations, the content of lead in released wastewater should be lower than 1.0 mg/L, whereas the lead content in wastewater from lead acid battery manufacturing is 2.2–97.7 mg/L. The lead

* Corresponding author.

content defined by the Environmental Quality Standard for soils is 35 mg/kg. However, the background value of lead in soil in China can be as high as 1,143 μg/L [6]. Therefore, research into high-efficiency and low-cost industrial wastewater treatment and soil recovery processes has crucial theoretical and practical value for the protection of the environment [7–10].

Many researchers have proven that natural or biowaste adsorbents have excellent adsorption effects on heavy metals, such as Pb, Cr, Cd and Zn [11–13]. Khan et al. [14] investigated the adsorption characteristics of Pb(II) onto multiwalled carbon nanotube-polyurethane (MWCNT/PU) in batch and fixed-bed experiments, and found that the adsorption capacity and breakthrough capacity reached 270.27 and 239.05 mg/g, respectively. Chaudhry et al. [15] reported that the adsorption capacity of Pb(II) onto manganese oxide-coated sand (MOCS) reached 147.06 ug/g at 40°C, and the adsorption process was exothermic and involved film diffusion. Khan and Singh [16] noted that the adsorption of Pb(II) onto clay is an endothermic process and exhibits good adsorption capacity, indicating that clay is a low-cost and good adsorbent for Pb(II) removal from wastewater. Furthermore, Khan et al. [17,18] found that fly ash and modified algal biomass are low-cost sorbents suitable for the adsorption of Pb(II) from wastewater, and the monolayer adsorption capacity reached 100.00 mg/g. However, the adsorption process is spontaneous and exothermic for fly ash, and spontaneous and endothermic for modified algal biomass. Sölener et al. [19] investigated the adsorption characteristics of clay-poly (methoxyethyl)acrylamide (PMEA) composites for Pb(II) and found a maximum adsorption capacity of 81.02 mg/g, and the adsorption equilibrium was reached within 60 min. Rakhym et al. [20] compared the adsorption capacities of Pb(II) on natural zeolite and chamotte clay and concluded that the maximum uptake of Pb(II) was 14 mg/g for zeolite and 11 mg/g for clay. For fine clay particles (effective diameter less than 1 μm), Yin et al. [21] found that the maximum adsorption capacities of Pb(II) onto cultivated loessial, dark loessial, manual loessial, and aeolian sandy were 588.24, 476.19, 416.67, and 263.16 mg/g, respectively. Based on batch experiments, Ahrouch et al. [22] reported that natural Moroccan clay is a cost-effective and potential adsorbent for Pb-contaminated wastewater, especially in developing regions. Sdiri et al. [23] indicated that the adsorption capacity for Pb(II) of Early Cretaceous clay was nearly 86.4 mg/g, and more than 95% of the adsorption occurred within 30 min. Humelnicu et al. [24] found that the maximum adsorption capacities of montmorillonite and aluminum-pillared clay were 92.59 mg/g for Cu(II), 97.08 mg/g for Pb(II), and 73.52 mg/g for Zn(II). Mu'azu [25] noted that the montmorillonite content of clay had a minor effect on the Pb(II) adsorption capacity, whereas it had a significant effect on that of Zn(II). Therefore, different montmorillonite contents may affect the adsorption properties and electrokinetic remediation process of clays. EI Batouti and Abouzeid [26] discovered that the Pb(II) adsorption capacity of Na-montmorillonite clay could be improved by pretreatment with HCl and HNO_3, and the optimum adsorption capacity was reached at pH 6 when using pretreated Na-montmorillonite as an adsorbent. Abdelwaheb et al. [27] concluded that the risk of groundwater contamination by

various pollutants followed the order $Pb^{2+} < Ni^{2+} < PO_4^{3-} < NO_3^-$ in sandy soil and $PO_4^{3-} < Pb^{2+} < Ni^{2+} < NO_3^-$ in clayey soil. Kushwaha et al. [28] found that the maximum adsorption capacities of natural clay and humic acid were 25.07 and 19.16 mg/g, respectively, suggesting that natural clay is a promising adsorbent for Pb(II) removal from soil and aquatic environments.

Kaolinite clay has the characteristics of cost effectiveness, a wide distribution, and a high specific surface area and exchange capacity and is therefore a potential adsorbent for the removal of heavy metals. Unuabonah et al. [29] studied the adsorption of Pb(II) and Cd(II) onto sodium tetraborate (NTB)-modified kaolinite clay and found that the NTB-modified kaolinite clay increased the adsorption of Pb(II) and Cd(II) by nearly 72.2% and 96.3%, respectively, compared to unmodified clay. Shahmohammadi-Kalalagh et al. [30] concluded that the adsorption capacities of Pb(II), Zn(II), and Cu(II) on kaolinite were 7.75, 4.95, and 4.42 mg/g, respectively, and the kinetics were more accurately predicted by a pseudo-second-order model than by a pseudo-first-order model. Fatimah [31] revealed that the adsorption capacity of kaolinite modified with 3-amino propyl trimethoxy silane (APTES) was approximately seven-fold higher than that of raw kaolinite, mainly due to the presence of chemical interactions on the surface of the modified kaolinite. Unuabonah et al. [32] indicated that the adsorption capacities of NTB-modified kaolinite clay reached 42.92 mg/g for Pb(II) and 44.05 mg/g for Cd(II), which were significantly higher than those of unmodified kaolinite clay. It can be concluded that modified kaolinite clay is a low-cost adsorbent that has potential applications for Pb(II) and Cd(II) removal. Jiang et al. [33] reported that when using kaolinite clay, the maximum adsorption amounts of Pb(II), Cd(II), Ni(II), and Cu(II) were reached within 30 min, and the Pb(II) concentration was reduced from 160.00 to 8.00 mg/L in real wastewater. EI-Naggar et al. [34] found that for kaolinite/smectite-A and kaolinite/smectite-B adsorbents, Pb removal increased with increasing initial concentration, contact time, and pH, and the reaction speed was high during the initial period and then decreased until reaching equilibrium at 45 and 30 min, respectively. Bahah et al. [35] concluded that the maximum adsorption capacity of Algerian kaolinite clay was 52.63 mg/g for Cu(II) and 57.30 mg/g for Pb(II), which indicated that kaolinite clay has a better affinity for Pb(II) than for Cu(II).

Bentonite clay is a promising adsorbent for the removal of heavy metal ions, and it has attracted scholarly interest. To investigate the factors influencing Cd, Cu, and Pb removal by Na-bentonite, Glatstein and Francisca [36] found that the ionic strength significantly affects Cd removal but has little effect on Pb and Cu removal. The test results indicated that Na-bentonite has a high adsorption capacity for Cd, Cu, and Pb. Meneguin et al. [37] studied the adsorption characteristics of Pb(II) and Cd(II) onto natural and calcium-calcined bentonite clay (CCBC) and concluded that the Langmuir model provided a good fit to the Pb(II) isotherm, and the Dubinin–Radushkevich model was suitable for fitting Cd(II). In addition, the pseudo-second-order model fit the kinetics of Pb(II) and Cd(II) well. Alexander et al. [38,39] investigated the adsorption characteristics of Pb(II), Cd(II), and Mn(II) on Dijah-Monkin bentonite clay

and concluded that the rate constant of Mn(II) is higher than that of Pb(II) in a multimetal system, whereas Pb(II) is preferably adsorbed to bentonite. Furthermore, they noted that the adsorption capacity of natural Nigerian bentonite is greater than that of calcined bentonite, and Pb(II) removal by natural bentonite reached 0.0448 mmol/g, which was significantly higher than the adsorption of Cd(II) and Mn(II). Perelomov et al. [40] concluded that the Pb(II) adsorption amount of Na-bentonite is higher than that of Al-bentonite, and this finding is consistent with the presence of lysine. Inglezakis et al. [41] concluded that the removal efficiency of Pb(II) by bentonite reached 90% at 60°C, while the removal efficiency by clinoptilolite was only 55%, indicating that the removal effect of Pb(II) by bentonite is better than that of clinoptilolite. Zou et al. [42] noted that the removal efficiency of Pb(II) onto magnetic bentonite (MB) reached 98.9% within 90 min for an initial Pb(II) concentration of 200 mg/L, and the maximum adsorption capacity reached 80.40 mg/g. Taha et al. [43] investigated the adsorption of heavy metal ions in polluted seawater onto Na-activated bentonite and found that the removal efficiencies for Pb(II), Cd(II), and Ni(II) were between 92% and 100%. Mo et al. [44] discovered that a granular composite adsorbent consisting of bentonite-polypropylene was effective in Pb(II) removal, suggesting that pore size enhancement is effective in increasing the adsorption capacity of granular bentonite composites. Awadh and Abdulla [45] found that the maximum Pb(II) adsorption capacity of Iraqi bentonite reached 0.6563 mg/g at 25°C and decreased to 0.5250 mg/g at 35°C, indicating that bentonite is a good natural adsorbent for Pb(II) removal. Graimed and Ali [46] reported that the maximum adsorption capacities of bentonite and activated carbon were 0.0364 and 0.015 mg/mg, respectively. Meanwhile, the adsorption process was endothermic and the kinetic results fit well with the pseudo-second-order model.

The adsorption performance of clay depends on its structure, and the structure of kaolinite clay is significantly different from that of bentonite clay. Kaolinite is a 1:1 dioctahedral clay mineral that has a two layered structure consisting of silicon-oxygen tetrahedral sheets linked to alumina octahedral sheets through –Al–O–H...O–Si–hydrogen bonding. The surface of one layer comprises basal oxygen atoms belonging to the tetrahedral sheet, while the other surface consists of OH groups from the octahedral sheet [47]. Bentonite is composed of units made up of two silica tetrahedral sheets with a central alumina octahedral sheet. The tetrahedral and octahedral sheets combine in such a way that the tips of the tetrahedra of each silica sheet and one of the hydroxyl layers of the octahedral sheet form a common layer. In addition, montmorillonite is the main component of bentonite [48,49]. Recent studies have indicated that clay has an excellent adsorption capacity for heavy metals, especially Pb(II). However, soil exhibits significant variations in physico-chemical properties and adsorption capacity. To date, few studies have compared Pb(II) adsorption between natural kaolinite and bentonite clays, especially the adsorption kinetics and thermodynamic characteristics. This study investigated the feasibility of using natural clays as cost-effective adsorbents for the removal of Pb(II) from aqueous solution. To achieve this aim, the adsorption kinetics, isothermal and thermodynamic

characteristics of Pb(II) were compared between natural kaolinite and bentonite clays, and the effects of the solid-to-liquid ratio, pH, temperature, and reaction time on the adsorption characteristics were analyzed. The research results can provide guidance for the practical engineering of treatment methods for Pb-containing wastewater.

2. Materials and methods

2.1. Materials

The kaolinite and bentonite used in this study were obtained from the Dalian and Heishan areas, respectively, in Liaoning Province, China. The air-dried kaolinite and bentonite were first crushed and placed in a 60°C oven (Shanghai Jinghong Laboratory Instrument Co., Ltd, China) for 24 h, then cooled to room temperature and passed through a 60-mesh geogrid. The meshed soils were stored in a desiccator before usage. The chemical compositions of the kaolinite and bentonite are listed in Table 1. The main chemical component of clays is SiO_2, and the mass of SiO_2, Al_2O_3, and Fe_2O_3 accounted for 85.80% and 87.94% of the kaolinite and bentonite clay, respectively. The pH values of the kaolinite and bentonite clay were 8.85, and 8.70, respectively, which were slightly alkaline. Based on Brunauer–Emmett–Teller (BET) analysis, the surface area, pore volume, and average pore size of the kaolinite clay were 14.96 m²/g, 0.028 cm³/g, and 7.89 nm, respectively. For bentonite clay, the surface area, pore volume, and average pore size were 31.36 m²/g, 0.074 cm³/g, and 7.75 nm, respectively. Based on the Standard for Soil Test Method (GBT 50123-2019), the density, liquid limit, and plastic limit for kaolinite clay were 1.65 g/cm³, 33.4%, and 17.1%, respectively, and the values for bentonite clay were 1.12 g/cm³, 99.7%, and 41.2%, respectively. Analytically pure $Pb(NO_3)_2$ (1.598 g) was dissolved in 1 L distilled water to prepare a 1,000 mg/L Pb(II) stock solution. The Pb(II) solutions used in this study were all prepared by diluting the stock solution with distilled water.

2.2. Batch tests

Erlenmeyer flasks with prepared samples were numbered and placed in a thermostatic oscillator (SHA-C,

Table 1
Chemical composition of kaolinite and bentonite

Kaolinite		Bentonite	
Chemical component	Mass (%)	Chemical component	Mass (%)
SiO_2	49.2	SiO_2	70.70
Al_2O_3	20.9	Al_2O_3	14.30
Fe_2O_3	15.7	Fe_2O_3	2.94
CaO	4.34	CaO	2.99
K_2O	4.09	K_2O	4.38
MgO	1.75	MgO	2.00
TiO_2	1.46	TiO_2	0.241
Na_2O	1.20	Na_2O	1.91
MnO	0.108	BaO	0.197

Guohua Electric Appliance Co., Ltd, China). The temperature was controlled according to the experimental conditions, and the oscillator operated at a rotation speed of 120 rpm for 12 h. The oscillation time was sufficient to reach adsorption equilibrium. After oscillation, the solution was centrifuged (CT15RT, Shanghai Tianmei Biochemical Equipment Engineering Co., Ltd., China) at 3,000 rpm for 10 min. The Pb(II) concentration and pH (pHe) in the supernatant were measured using an atomic absorption spectrophotometer (AA6000, Shanghai Tian Mei Biochemical Engineering Equipment Co., Ltd., China) and a pH meter (Starter 2C, Ohaus Instruments (Shanghai) Co., Ltd., USA), respectively.

The adsorption capacity q_t (mg/g), removal rate R (%), and solid-to-liquid ratio r (g/L) at equilibrium were calculated using the Eqs. (1)–(3) [25,42]

$$q_t = \frac{(C_0 - C_t)}{m} \times V \tag{1}$$

$$R(\%) = \frac{(C_0 - C_e)}{C_0} \times 100 \tag{2}$$

$$r = \frac{m}{V} \tag{3}$$

where C_0 is the Pb(II) concentration at the initial time, C_t is the Pb(II) concentration at time t, C_e is the Pb(II) concentration at the equilibrium time (mg/L), V is the volume of solution (L), and m is the mass of kaolinite or bentonite (g).

2.3. Theoretical models

2.3.1. Adsorption isotherm models [27,43]

In this paper, the Langmuir model, Freundlich model and Dubinin–Radushkevich (D-R) model were used to fit the isothermal adsorption test data, and the adsorption characteristics of Pb(II) on the two adsorbents were analyzed.

2.3.1.1. Langmuir model

$$\frac{C_e}{q_e} = \frac{1}{bQ} + \frac{C_e}{Q} \tag{4}$$

where C_e is the equilibrium concentration of Pb(II) (mg/L), q_e is the adsorption capacity at equilibrium (mg/g), Q is the single-layer maximum adsorption capacity (mg/g) of the adsorbent, and b is the Langmuir model constant (L/mg).

$$R_L = \frac{1}{1 + bC_0} \tag{5}$$

where R_L is the separation factor (dimensionless), b is the Langmuir model constant (L/mg), and C_0 is the initial concentration of Pb(II) (mg/L).

The value of R_L can indicate whether the adsorption reaction is favorable. When $0 < R_L < 1$, the adsorption reaction is favorable; when $R_L > 1$, it is unfavorable. When $R_L = 1$, the adsorption is reversible; when $R_L = 0$, it is irreversible [20].

2.3.1.2. Freundlich model

$$\log q_e = \log K_F + \frac{1}{n} \log C_e \tag{6}$$

where q_e is the adsorption capacity at equilibrium (mg/g), C_e is the equilibrium concentration of Pb(II) (mg/L), K_F is the model constant related to the adsorption capacity (mg/g), and n is the model constant related to adsorption strength (dimensionless).

2.3.1.3. Dubinin–Radushkevich (D-R) model

$$\ln q_e = \ln q_m - k\varepsilon^2 \tag{7}$$

where q_e is the adsorption capacity at equilibrium (mg/g), q_m is the maximum adsorption capacity (mol/g), k is the model constant related to free energy (mol²/kJ²), and ε is the Polanyi potential (kJ/mol).

$$E = -\frac{1}{\sqrt{2k}} \tag{8}$$

where E is the average adsorption free energy (kJ/mol), and k is the model constant (mol²/kJ²).

When $1.0 < |E| < 8.0$ kJ/mol, the adsorption mechanism is physical adsorption; when $8.0 < |E| < 16.0$ kJ/mol, the adsorption mechanism is ionic exchange.

2.3.2. Adsorption kinetic models [30,34]

According to different adsorption mechanisms and assumption conditions, several adsorption kinetic models were applied to study the adsorption process of the adsorbate onto the adsorbent and the rate of adsorption.

2.3.2.1. Pseudo-first-order kinetic model

$$\log(q_e - q_t) = \log q_e - \frac{k_1}{2.303} t \tag{9}$$

where q_t and q_e are the adsorption capacity (mg/g) at time t and at equilibrium, respectively, and k_1 is the adsorption rate constant of pseudo-first-order kinetics (1/min).

2.3.2.2. Pseudo-second-order kinetic model

$$\frac{t}{q_t} = \frac{1}{k_2 q_e^2} + \frac{t}{q_e} \tag{10}$$

where q_t and q_e are the adsorption capacity (mg/g) at time t and at equilibrium, respectively, and k_2 is the adsorption rate constant of pseudo-second-order kinetics (g/mg/min).

When t approaches 0, h can be expressed as:

$$h = k_2 q_e^2 \tag{11}$$

where k_2 is the adsorption rate constant (g/mg/min), q_e is the adsorption capacity at equilibrium (mg/g), and h is the initial adsorption rate (mg/g/min).

2.3.2.3. Internal diffusion model

$$q_t = k_{int} t^{1/2} + c \tag{12}$$

where q_t is the adsorption capacity (mg/g), k_{int} is the internal diffusion rate constant (mg/g/min$^{1/2}$), and c is the intercept which is related to the thickness of the boundary layer (dimensionless).

2.3.3. Adsorption thermodynamic model [38]

The adsorption thermodynamic equations can be expressed as

$$K_D = \frac{q_e}{C_e} \tag{13}$$

$$\ln K_D = \frac{\Delta S}{R} - \frac{\Delta H}{RT} \tag{14}$$

$$\Delta G = \Delta H - T\Delta S \tag{15}$$

where K_D is the distribution coefficient at the solid-liquid interface (mL/g), q_e is the adsorption capacity at equilibrium (mg/g), C_e is the equilibrium concentration of Pb(II) (mg/L), R is the molar gas constant (8.314 J/mol/K), T is the thermodynamic temperature (K), ΔS is the entropy change (J/mol/K), ΔH is the enthalpy change (kJ/mol), and ΔG is the Gibbs free energy (kJ/mol).

3. Results and discussion

3.1. Effect of the solid-to-liquid ratio on adsorption

The effects of the solid-to-liquid ratio on the adsorption capacity of Pb(II) at 30°C were investigated for different adsorbents. As shown in Fig. 1a, the initial concentrations of Pb(II) were 50, 100, and 150 mg/L, and the solid-to-liquid ratio changed from 4 to 40 g/L. The data show that the adsorption capacity of Pb(II) on kaolinite gradually decreases as the solid-to-liquid ratio increases, and the initial concentration of Pb(II) significantly affects the adsorption capacity [43]. As the kaolinite content increases, an increase in the number of active adsorption sites on the surface of the clay results in an increase in the removal rate. An increase in the amount of clay results in the agglomeration of soil particles, which causes a decrease in the total surface area and an increase in the diffusion path length, therefore resulting in a decrease in the adsorption capacity [32]. As shown in Fig. 1b, the initial concentrations of Pb(II) were 300, 350, and 400 mg/L with varying solid-to-liquid ratios from 2 to 40 g/L. At initial concentrations of 300, 350, and 400 mg/L, the adsorption capacity reaches its peak value at solid-to-liquid ratios of 6, 8, and 10 g/L, respectively. To the left of the peak value, the adsorption capacity increases as the solid-to-liquid ratio increases. The maximum adsorption capacity is attained at an initial Pb(II) concentration of 300 mg/L. To the right of the peak value, the adsorption capacity decreases as the solid-to-liquid ratio increases. The minimum adsorption capacity is reached at an initial Pb(II) concentration of 300 mg/L. At a low solid-to-liquid ratio, Pb(II) is easier to hydrolyze at higher initial concentrations, and the pH of the solution is lower. Changes on the left side of the peak value are primarily related to the pH of the solution. At a high solid-to-liquid ratio, the increase in bentonite content causes the agglomeration of soil particles, resulting in a decrease in the total surface area and an increase in the diffusion path length; therefore, the adsorption capacity decreases.
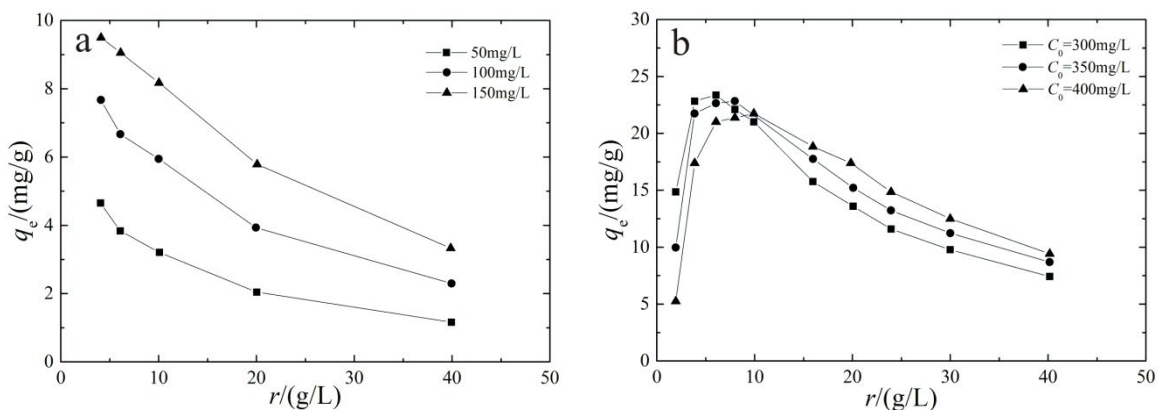
Fig. 1. Effect of solid-to-liquid ratio on Pb(II) adsorption of (a) kaolinite and (b) bentonite (pH 6.0, temperature 30°C, and reaction time 120 min).

3.2. Effect of pH_0 on the removal rate

Variations in solution pH strongly affect the adsorption process for the removal of metal ions from wastewater [35]. Visual MINTEQ v2.6.1 software was used to calculate the forms of Pb(II) at different pH_0 values. Pb(II) primarily exists as Pb^{2+} at $pH_0 < 6.0$; when $6.0 < pH_0 < 9.0$, the concentration of Pb^{2+} dramatically decreases; $Pb(OH)^+$ and $Pb_3(OH)_4^{2+}$ form at $pH_0 > 6.0$; and the concentration of $Pb(OH)^+$ reaches its peak value at $pH_0 = 7.5$. The concentration of $Pb_3(OH)_4^{2+}$ gradually increases at $pH_0 > 7.25$ and reaches its peak value at $pH_0 = 9.25$; $Pb(OH)_2$ begins to form at $pH_0 > 8.0$ and reaches its peak concentration at $pH_0 = 11.0$. To investigate the adsorption characteristics of Pb(II) onto kaolinite and bentonite, pH_0 was maintained below 6 in the experiments. As shown in Fig. 2a, an initial concentration of Pb(II) of 300 mg/L, solid-to-liquid ratio of 7.5 g/L, ionic strength of 0.001 mol/L, and varying pH_0 values to analyze the corresponding changes in the removal rate. The removal rate was less than 10% at $pH_0 < 1.7$; when $pH_0 = 2.4$, the removal rate reached 83.92%; and the rate approached 100% at $pH_0 = 2.91–6.0$. Therefore, maintaining pH_0 in the range of 2.91–6.0 can effectively increase the removal of Pb(II) in wastewater. As shown in Fig. 2b, an initial Pb(II) concentration of 400 mg/L, solid-to-liquid ratio of 10 g/L, and ionic strength of 0.001 mol/L. The removal rate rapidly increased as pH_0 increased from 2 to 7 and nearly unchanged when $pH_0 > 7$ [43], which showed inconsistent with the results of Iraqi bentonite [45].

Kaolinite contains amphiphilic functional groups (hydroxyl groups on the edge or surface of the clay minerals) and an alkaline component (CaO). pH affects the form of the ions, the degree of ionization at adsorption sites, and the charge on the surface of the adsorbent. The effect of pH on Pb(II) removal by kaolinite can be summarized as follows:

• At $pH_0 < 1.7$, adsorption sites on the surface of kaolinite are occupied by large amounts of H^+, which inhibits the approach of Pb^{2+} and decreases the possibility of Pb^{2+} adsorption on the surface of kaolinite, resulting in a lower removal rate of Pb(II). As pH_0 increases, the concentration of H^+ in the solution decreases, and the competition between H^+ and Pb^{2+} decreases, thus increasing the removal rate of Pb(II).

• At $pH_0 < pH_{pzc} = 2.03$, the surface of kaolinite is positively charged due to the adsorption of H^+. Therefore, electrostatic repulsion exists between kaolinite and Pb(II), where a lower pH_0 promotes stronger repulsion. At $pH_0 > pH_{pzc}$, the surface of kaolinite is negatively charged due to H^+ ionization. Electrostatic attraction exists between kaolinite and Pb(II) as follows:

$$\equiv S-OH_2^+ \leftrightarrow \equiv SOH + H^+ \tag{16}$$

$$\equiv S-OH \leftrightarrow \equiv SO^- + H^+ \tag{17}$$

where $\equiv S$ represents Si or Al adsorption sites on the surface of kaolinite, and $\equiv S-OH_2^+$, $\equiv S-OH$, and $\equiv S-O^-$ are protonated, neutral, and deprotonated hydroxyls.

The measurement of the aqueous kaolinite solution is $pH_{na} = 8.86 > pH_{pzc} = 2.03$, which indicates that Pb(II) can adsorb onto kaolinite. The data in Fig. 2a show that at $pH_0 < 2$, the removal rate of Pb(II) by kaolinite is low, and the mechanism of Pb(II) adsorption onto kaolinite is ionic exchange. With a gradual increase in pH_0, the ionization degree of the kaolinite surface increases, and deprotonated hydroxyl groups form complexes with Pb^{2+} that are adsorbed onto the negatively charged adsorption sites on the kaolinite surface through electrostatic attraction. The interaction between the heavy metal Pb^{2+} and the minerals in kaolinite is as follows [50].

$$2\left(\equiv XNa/H\right) + Pb^{2+} \leftrightarrow \left(\equiv X\right)_2 Pb + 2Na^+/H^+ \tag{18}$$

$$\equiv S-OH + Pb^{2+} \leftrightarrow \equiv SOPb^+ + H^+ \tag{19}$$

$$2 \equiv S-O^- + Pb^{2+} \rightarrow \equiv SO^-PbOS \equiv \tag{20}$$
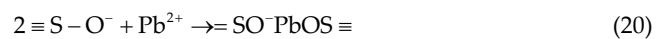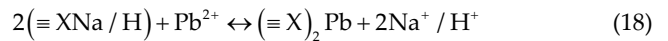
where $\equiv X$ is an ionic exchange site on the surface of the adsorbent.
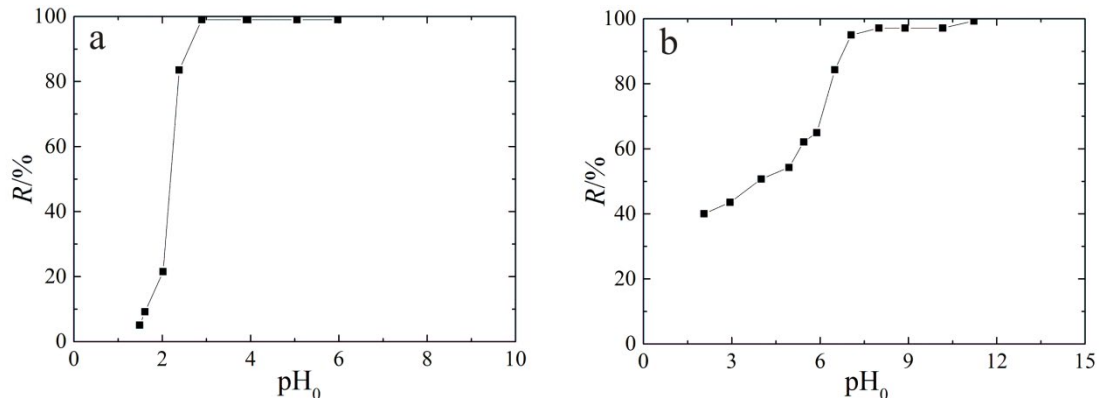
Fig. 2. Effect of pH on Pb(II) removal by (a) kaolinite (initial concentration 300 mg/L, solid-to-liquid ratio 7.5 g/L, temperature 30°C, and reaction time 120 min) and (b) bentonite (initial concentration 400 mg/L, solid-to-liquid ratio 10.0 g/L, temperature 30°C, and reaction time 120 min).

For bentonite, Pb(II) exists in solution as Pb^{2+}, and the removal of Pb(II) by bentonite occurs via adsorption at $pH_0 < 7$. The primary adsorption mechanism is ionic exchange, that is, H^+/Na^+ on the exchangeable adsorption sites of bentonite is replaced by an equivalent amount of Pb^{2+} from the solution. At $pH_0 = 7–10$, $Pb(OH)^+$ and $Pb(OH)_2$ are the primary forms of Pb(II) in the solution. The removal of Pb(II) by bentonite includes the adsorption of $Pb(OH)^+$ and the precipitation of $Pb(OH)_2$. When $pH_0 > 10$, $Pb(OH)_2$ and $Pb(OH)_3^-$ are the primary forms of Pb(II) in the solution, and the removal of Pb(II) by bentonite is primarily from the precipitation of $Pb(OH)_2$. At $pH_0 < 7$, the removal of Pb(II) by bentonite is significantly affected by the concentration of NaCl, indicating that the primary adsorption mechanism is ionic exchange (or complex formation on the outer surface). At $7 < pH_0 < 10$, the removal of Pb(II) by bentonite is independent of the concentration of NaCl, indicating that the removal mechanism is primarily complex formation on the internal surface. The formulas for hydrolysis and chemical precipitation are as follows [51].

$$Pb^{2+} + H_2O \leftrightarrow Pb(OH)^+ + H^+ \tag{21}$$

$$Pb(OH)^+ + H_2O \leftrightarrow Pb(OH)_2(s) + H^+ \tag{22}$$
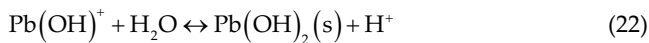
3.3. Adsorption kinetic characteristics

To investigate the adsorption kinetic characteristics of Pb(II) onto kaolinite and bentonite, experiments were conducted at initial Pb(II) concentrations of 200, 250, and 300 mg/L and a solid-to-liquid ratio of 10 g/L for kaolinite. As shown in Fig. 3a, the adsorption of Pb(II) onto kaolinite is a rapid process that reaches adsorption equilibrium within 120 min. The first 15 min is the rapid adsorption phase, which is consistent with the results for NTB-modified kaolinite clay [29]. With a high concentration of Pb(II), the diffusion rate of Pb(II) to the adsorption sites on the clay surface is rapid, and the adsorption rate is high. As the reaction time increases, the concentration of Pb(II) in the solution decreases, and the adsorption sites on the clay surface become saturated. As the concentration difference between the soil and solution decreases, the diffusion rate of the clay particles decreases, and the adsorption rate also decreases. For bentonite, the initial concentrations were 200, 250, and 300 mg/L, and the solid-to-liquid ratio was 5 g/L. The dependence of the adsorption ability for Pb(II) of bentonite on reaction time is shown in Fig. 3b. The removal of Pb(II) by bentonite is a rapid adsorption process, in which the removal rate reaches 50% in 15 min and the equilibrium state is reached within 120 min [45,46]. This rapid adsorption phenomenon indicates that the removal of Pb(II) by bentonite is a chemical adsorption process and not a physical adsorption process.

To describe the characteristics of the adsorption kinetics of Pb(II) onto kaolinite and bentonite, the pseudo-first-order kinetic model, pseudo-second-order kinetic model, and internal diffusion model were used to analyze the experimental data. The results are shown in Figs. 4 and 5. The model parameters of the kinetic model and the coefficients of determination are listed in Table 2. It can be concluded that the pseudo-second-order kinetic model is more suitable than other models for simulation the characteristics of the adsorption kinetics of Pb(II) onto clays [19,22,37]. The internal diffusion model shows that the total adsorption rate is controlled by both surface adsorption (liquid film diffusion) and particle internal diffusion. Clay is a porous medium; therefore, its adsorption process includes three continuous steps. The first step is the surface adsorption phase, where Pb(II) diffuses to the outer surface of the clay through the liquid film. The second-step is the gradual adsorption phase, where the internal diffusion within the particles is the rate-limiting step. The third step is the equilibrium phase, where the residual Pb(II) concentration decreases, the internal diffusion rate in the particles also decreases, and the adsorption reaction reaches equilibrium. In Table 2, the thickness of the boundary layer (c_2) of particle internal diffusion is larger than that of liquid film diffusion (c_1). Therefore, the liquid film diffusion rate (k_{i1}) is significantly higher than the particle internal diffusion rate (k_{i2}).

For bentonite, a higher initial concentration of 300 mg/L results in a larger gradient between the soil and the water,
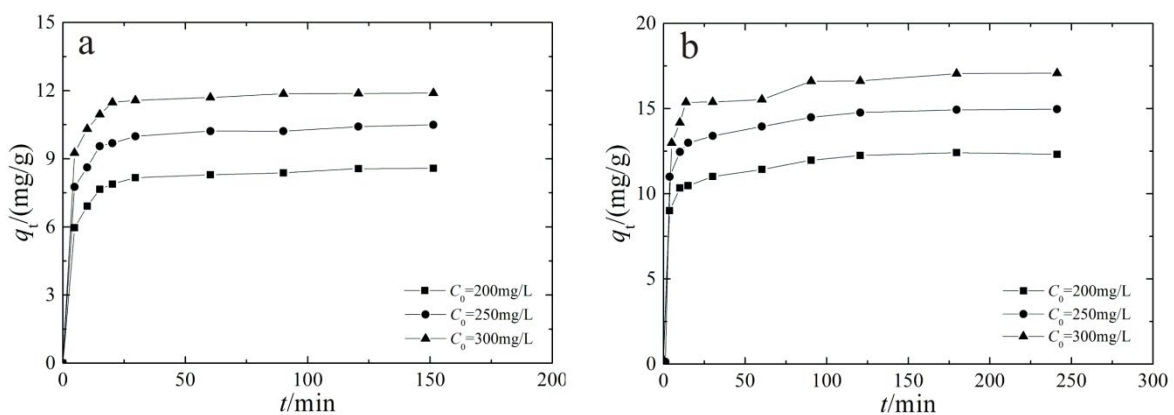
Fig. 3. Effect of reaction time on Pb(II) adsorption by (a) kaolinite (solid-to-liquid ratio 10.0 g/L, pH 6.0, and temperature 30°C) and (b) bentonite (solid-to-liquid ratio 5.0 g/L, pH 6.0, and temperature 30°C).
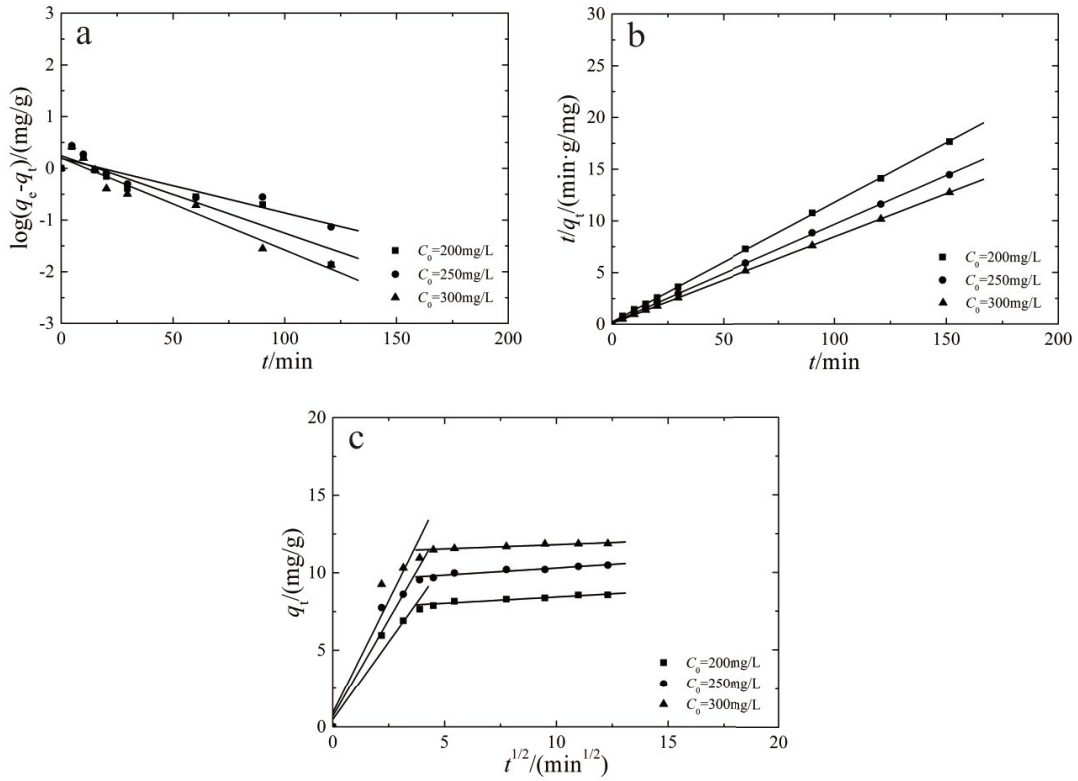
Fig. 4. Fitting curves of the kinetic model for Pb(II) adsorption onto kaolinite (a) pseudo-first-order kinetics model, (b) pseudo-second-order kinetics model and (c) intraparticle diffusion model (solid-to-liquid ratio 10.0 g/L, pH 6.0, and temperature 30°C).
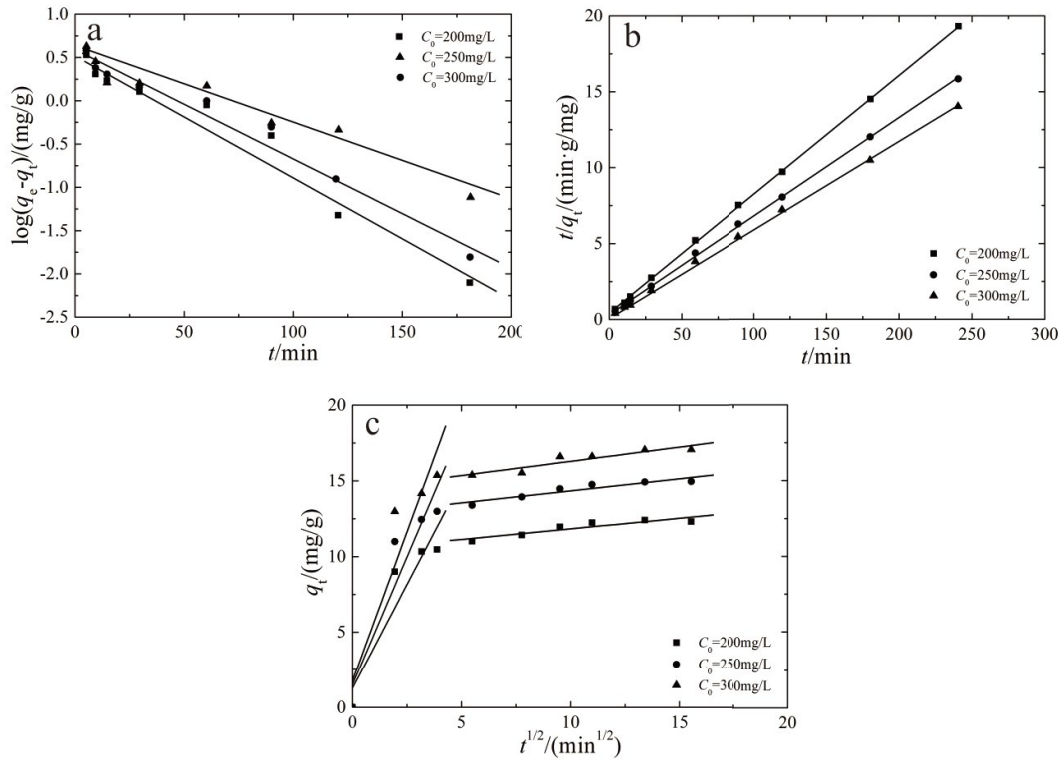
Fig. 5. Fitting curves of the kinetic model for Pb(II) adsorption onto bentonite (a) pseudo-first-order kinetics model, (b) pseudo-second-order kinetics model and (c) intraparticle diffusion model (solid-to-liquid ratio 5.0 g/L, pH 6.0, and temperature 30°C).

Table 2
Model parameters of the adsorption kinetic models

Model	Parameters	Kaolinite			Bentonite		
		200 mg/L	250 mg/L	300 mg/L	200 mg/L	250 mg/L	300 mg/L
Pseudo-first-order kinetic model	q_e (mg/g)	1.7482 ± 0.1181	1.5557 ± 0.0896	1.5908 ± 0.0965	3.7427 ± 0.1018	3.9793 ± 0.0747	3.4652 ± 0.0756
	$k_1 \times 10^{-3}$ (1/min)	34.43 ± 2.12	24.27 ± 1.61	41.04 ± 1.73	32.86 ± 1.17	28.86 ± 1.99	19.62 ± 2.00
	R^2	0.9363	0.9274	0.9685	0.9803	0.9861	0.9701
Pseudo-second-order kinetic model	q_e (mg/g)	8.6520 ± 0.0459	10.5374 ± 0.0352	11.9703 ± 0.0180	12.7307 ± 0.0475	15.4536 ± 0.0523	17.3913 ± 0.0513
	$k_2 \times 10^{-3}$ (g/mg/min)	62.72 ± 0.01	59.85 ± 0.01	78.91 ± 0.01	15.22 ± 0.01	11.77 ± 0.01	13.39 ± 0.01
	R^2	0.9999	0.9999	0.9999	0.9999	0.9998	0.9998
Internal diffusion model	k_{i1} (mg/g/min$^{1/2}$)	2.0152 ± 0.3280	2.5093 ± 0.4717	2.9152 ± 0.6155	2.7532 ± 0.7468	3.3824 ± 0.8852	3.9442 ± 1.0390
	c_1	0.4856 ± 0.0280	0.6966 ± 0.0717	0.9108 ± 0.0955	1.2634 ± 0.7468	1.5043 ± 0.8852	1.7641 ± 1.0390
	R_1^2	0.9745	0.9664	0.9582	0.9337	0.9378	0.9371
	k_{i2} (mg/g/min$^{1/2}$)	0.0816 ± 0.0122	0.0911 ± 0.0147	0.0547 ± 0.0070	0.1398 ± 0.0312	0.1595 ± 0.0302	0.1881 ± 0.0376
	c_2	7.6243 ± 0.0122	9.3993 ± 0.0147	11.2675 ± 0.0070	10.4359 ± 0.0312	12.7466 ± 0.0302	14.4117 ± 0.0376
	R_2^2	0.9578	0.9515	0.9691	0.9131	0.9353	0.9285

a stronger driving force for diffusion toward the surface of the soil particles, and a greater equilibrium adsorption capacity. However, the results from the pseudo-first-order kinetic model show that the equilibrium adsorption capacity is the smallest for the initial concentration of 300 mg/L, indicating that the pseudo-first-order kinetic model does not accurately reflect the kinetic process of the adsorption of Pb(II) onto bentonite. At initial concentrations of 200, 250, and 300 mg/L, the coefficients of determination fitted by the pseudo-first-order kinetic model are 0.9803, 0.9861, and 0.9701, respectively. The corresponding coefficients of determination fitted by the pseudo-second-order kinetic model are 0.9999, 0.9998 and 0.9998. Both models have a high coefficient of determination, while the calculated values from the pseudo-second-order kinetic model fit the measured values better; therefore, the pseudo-second-order kinetic model better explains the adsorption kinetic phenomena. There are two reasons why the pseudo-first-order kinetic model does not accurately describe the adsorption kinetic process [52].

- The expression $k_1 (q_e - q_t)$ does not completely represent all of the effective adsorption sites in bentonite. Therefore, it is only suitable for describing the adsorption at the initial stage.
- If the intercepts of $\lg q_e$ and the line $\lg(q_e - q_t)$–t are not equal, the experimental q_e used in the fitting of $\lg(q_e - q_t)$ may be different from the real value. However, the pseudo-second-order kinetic model can accurately describe the overall process of adsorption, such as external liquid film diffusion, surface adsorption, and particle internal diffusion, which further proves that the adsorption of Pb(II) onto bentonite is a chemical adsorption process [53].

The adsorption rate constants calculated from the pseudo-first-order and pseudo-second-order kinetic models both decrease as the initial concentration increases. The primary reason is that a higher initial concentration results in a longer time for the soil-water interface to reach equilibrium, which lowers the adsorption rate constant. Similar to kaolinite, bentonite is also a porous medium, and its adsorption process includes three continuous steps, namely, the surface adsorption phase, gradual adsorption phase, and equilibrium phase. The internal diffusion rate in the particle also decreases, and the adsorption reaction reaches equilibrium. In Table 2, the thickness of the boundary layer (c_2) in particle internal diffusion is greater than that of the liquid film diffusion (c_1). Therefore, the liquid film diffusion rate (k_{i1}) is significantly higher than the particle internal diffusion rate (k_{i2}).

3.4. Adsorption isotherm characteristics

The isothermal adsorption characteristics were investigated at temperatures of 20°C, 30°C, and 40°C, and the results are shown in Fig. 6. For kaolinite, isothermal adsorption tests were carried out under the conditions of a solid-to-liquid ratio of 6 g/L, and initial Pb(II) concentrations in the range of 20 to 300 mg/L. For bentonite, isothermal adsorption tests were carried out under the conditions of

a solid-to-liquid ratio of 10 g/L and initial Pb(II) concentrations in the range of 50 to 500 mg/L. According to the classification of isothermal adsorption curves by Giles and Smith, the isothermal adsorption curves of Pb(II) onto kaolinite and bentonite at different temperatures are all L-type curves. As the Pb(II) concentration in the solution increases, the slope of the curve gradually decreases, showing the high affinity of kaolinite to low-concentration Pb(II), which is consistent with the results for Algerian clay [35]. The adsorption capacity of Pb(II) on kaolinite decreases as the temperature increases, indicating that the adsorption is an exothermic process. However, the adsorption capacity

on bentonite gradually increases with temperature, which reveals that the adsorption process of Pb(II) onto bentonite is an endothermic process. The enhancement of adsorption capacity with increasing temperature could result from increased mobility and diffusion of ionic species [46].

To study the adsorption characteristics of Pb(II) onto kaolinite and bentonite, the Langmuir model, Freundlich model, and Dubinin–Radushkevich (D-R) model were used to fit the isothermal data using the least squares method, and the results are shown in Figs. 7 and 8. Model parameters and coefficients of determination are listed in Table 3. The Langmuir model simulates the isothermal adsorption
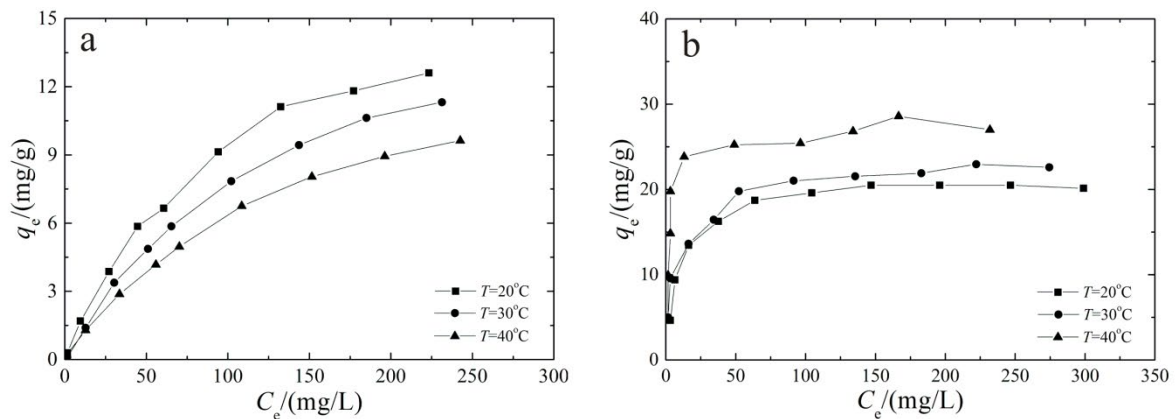
Fig. 6. Isothermal adsorption curves of Pb(II) at different temperatures (a) kaolinite (solid-to-liquid ratio 6.0 g/L, pH 6.0, and reaction time 120 min) and (b) bentonite (solid-to-liquid ratio 10.0 g/L, pH 6.0, and reaction time 120 min).
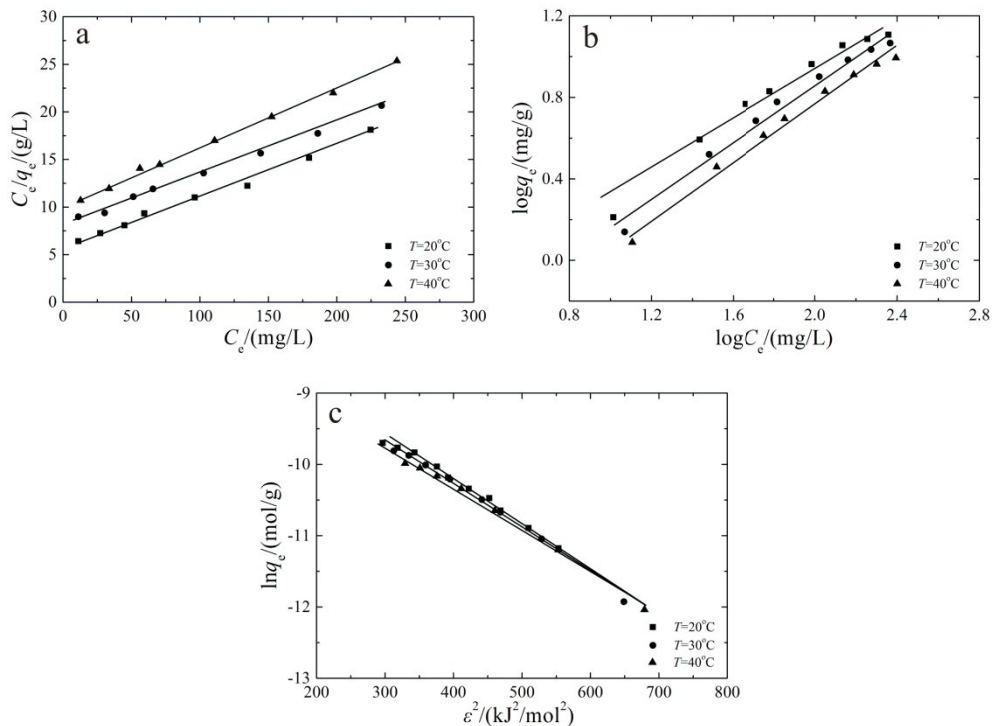
Fig. 7. Fitting curves of the isotherm model for Pb(II) adsorption onto kaolinite (a) Langmuir model, (b) Freundlich model, and (c) D-R model (solid-to-liquid ratio 6.0 g/L, pH 6.0, and reaction time 120 min).
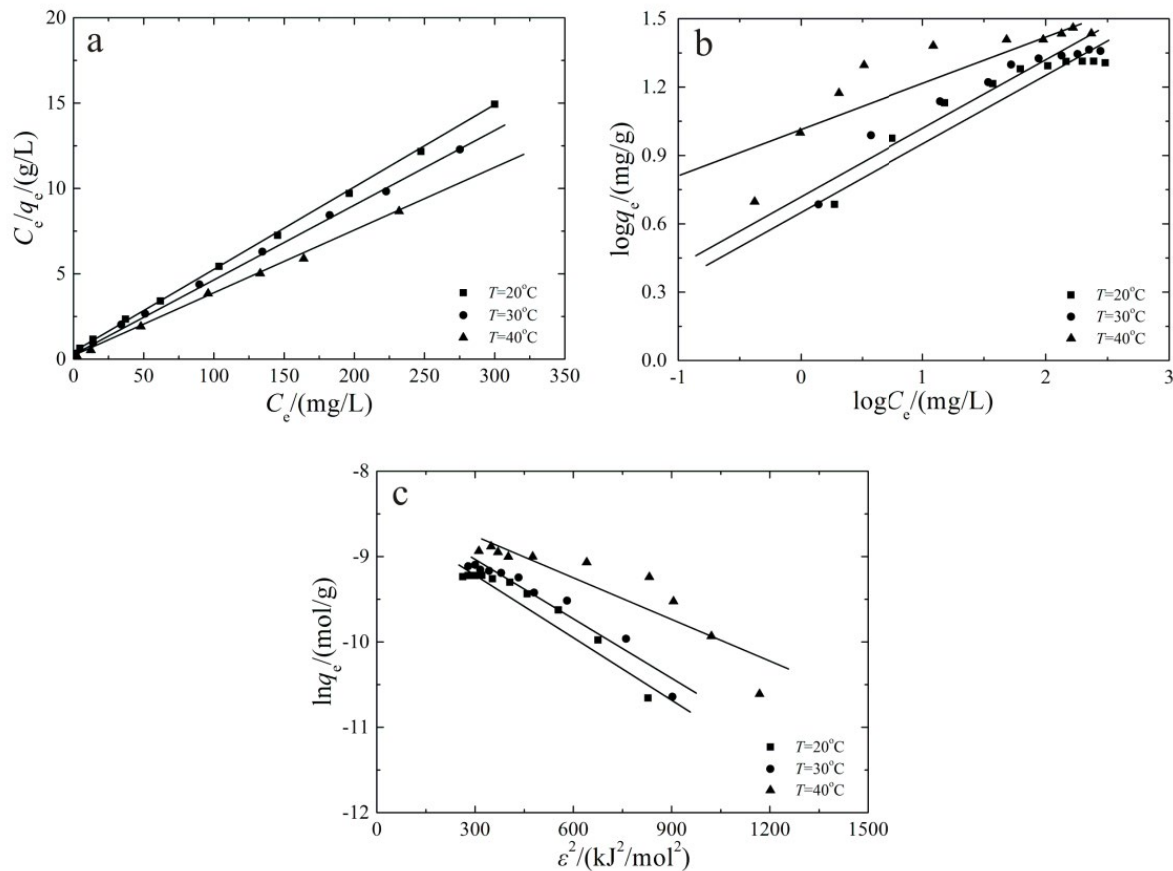
Fig. 8. Fitting curves of the isotherm model for Pb(II) adsorption onto bentonite (a) Langmuir model, (b) Freundlich model, and (c) D-R model (solid-to-liquid ratio 10.0 g/L, pH 6.0, and reaction time 120 min).

Table 3
Model parameters of the isothermal adsorption models

Model	Parameters	Kaolinite			Bentonite		
		20°C	30°C	40°C	20°C	30°C	40°C
Lang-muir	Q (mg/g)	18.8573 ± 0.2266	17.0295 ± 0.1653	16.1264 ± 0.1705	20.9820 ± 0.0596	23.2019 ± 0.0704	27.2257 ± 0.0968
	b (L/mg)	0.0092 ± 0.0019	0.0064 ± 0.0013	0.0062 ± 0.0013	0.1030 ± 0.0063	0.1503 ± 0.0069	0.3606 ± 0.0080
	R_L	0.8453	0.8864	0.8904	0.1627	0.1062	0.0525
	R^2	0.9963	0.9982	0.9987	0.9998	0.9996	0.9989
Freun-dlich	K_F (mg/g)	0.4052 ± 0.0850	0.2749 ± 0.0724	0.2300 ± 0.0641	5.5228 ± 0.0608	5.9204 ± 0.0518	10.3455 ± 0.0625
	n	1.4991 ± 0.0453	1.4066 ± 0.0380	1.4223 ± 0.0331	3.8405 ± 0.0332	3.7401 ± 0.0290	4.6679 ± 0.0407
	R^2	0.9864	0.9916	0.9934	0.9408	0.9560	0.8807
D-R	q_m (mol/g)	91.8348 ± 0.0850	89.8742 ± 0.0877	71.3137 ± 0.0847	43.2754 ± 0.1149	47.4188 ± 0.1046	53.7842 ± 0.1872
	$k \times 10^{-3}$ (mol²/kJ²)	6.31 ± 0.20	6.34 ± 0.20	5.96 ± 0.18	2.41 ± 0.24	2.28 ± 0.20	1.65 ± 0.26
	E (kJ/mol)	−8.9017	−8.8806	−9.1593	−14.4016	−14.8143	−17.4135
	R^2	0.9954	0.9972	0.9977	0.9622	0.9701	0.9101

characteristics of Pb(II) onto kaolinite better than the other two models [28]. By calculation, $0 < R_L < 1$ and $1 < n < 10$ are obtained for different temperatures, which indicates that the adsorption of Pb(II) onto kaolinite is favorable [19]. At 20°C, 30°C, and 40°C, the model parameter Q from the

Langmuir model, K_F from the Freundlich model and q_m from the D-R model decrease as the temperature increases, which indicates that the adsorption of Pb(II) onto kaolinite is an exothermic process and that low temperature is favorable for the adsorption of Pb(II). When the temperature

increases from 20°C to 40°C, the average adsorption free energies are –8.90, –8.88, and –9.16 kJ/mol, which demonstrates that the adsorption mechanism of Pb(II) onto kaolinite is ionic exchange. For bentonite, the coefficients of determination from the Langmuir model are higher than those of the Freundlich and D-R models, indicating that the Langmuir model is more suitable for describing the isothermal adsorption process of Pb(II) onto bentonite. The Freundlich model is unable to predict the maximum adsorption capacity, while the Langmuir and D-R models can. The adsorption capacity of bentonite increases exponentially as the Pb(II) concentration in solution increases, and there is no peak value. Therefore, the Freundlich model does not accurately describe the isothermal adsorption process of Pb(II) onto bentonite. $1 < n < 10$ occurs at different temperatures, further indicating that bentonite is suitable for Pb(II) adsorption [43]. $0 < R_L < 1$ was obtained at all different temperatures and initial Pb(II) concentrations, indicating that bentonite is suitable for Pb(II) adsorption [42]. At a constant temperature, R_L approaches 0 as the initial concentration increases, indicating that bentonite has a high affinity for low-concentration Pb(II). In this analysis, b is a constant that is related to the heat of adsorption. In this endothermic reaction, b increases with temperature. Therefore, at the same initial concentration, R_L decreases as the temperature increases. At the same temperature, the q_m value calculated from the D-R model is higher than the single layer adsorption capacity calculated from the Langmuir

model. This is because the Langmuir model is based on mono molecule layer adsorption, while the D-R model is based on the assumption that the adsorbent pores become filled with solute [42]. The maximum adsorption capacities calculated by the Langmuir model and the D-R model are larger than the experimental values. These results indicate that the Langmuir model and the D-R model represent ideal conditions, which is rarely the case in practical applications. When the temperature increases from 20 to 40°C, the average adsorption free energies are –14.40, –14.81, and –17.41 kJ/mol, indicating that at 20°C and 30°C, the primary adsorption mechanism of Pb(II) onto bentonite is ionic exchange. At 40°C, the adsorption of Pb(II) onto bentonite is a chemical adsorption process. A temperature increase can activate adsorption sites on the surface of bentonite, thus increasing the number of adsorption sites while decreasing the activation energy of the reaction. These conditions are beneficial to the formation of chemical bonds and chemical adsorption.

3.5. Thermodynamic characteristics

The thermodynamic characteristics of Pb(II) adsorption onto kaolinite and bentonite were investigated by varying the temperature and the initial concentration, and the results are listed in Table 4. For kaolinite, when the initial concentration of Pb(II) increases from 20 to 200 mg/L, the Gibbs free energies are all negative, indicating that the adsorption reaction

Table 4
Model parameters of the thermodynamics model

Adsorbents	C_0 (mg/L)	T (K)	ΔG (kJ/mol)	ΔH (kJ/mol)	ΔS (J/mol/K)	R^2
Kaolinite	20	293	–13.2632	–25.5653 ± 0.6892	–41.9864 ± 0.0762	0.9582
		303	–12.8434			
		313	–12.4235			
	50	293	–13.1775	–28.5296 ± 0.7564	–52.3963 ± 0.0796	0.9136
		303	–12.6535			
		313	–12.1295			
	150	293	–12.3283	–29.8665 ± 0.7961	–59.8571 ± 0.0842	0.8484
		303	–11.7298			
		313	–11.1312			
	200	293	–12.0369	–29.8757 ± 0.8064	–60.8832 ± 0.8319	0.8657
		303	–11.4281			
		313	–10.8193			
Bentonite	50	293	–34.8343	26.7673 ± 0.9611	210.2442 ± 1.1376	0.8304
		303	–36.9367			
		313	–39.0392			
	100	293	–34.5159	54.9067 ± 1.4325	305.1964 ± 1.7329	0.9997
		303	–37.5678			
		313	–40.6198			
	150	293	–32.4992	64.4246 ± 1.7538	330.7978 ± 1.9089	0.8597
		303	–35.8072			
		313	–39.1151			
	200	293	–30.6263	99.5231 ± 2.0357	444.1962 ± 2.0506	0.8734
		303	–35.0683			
		313	–39.5103			

is a spontaneous process [35,37,38]. As the temperature and initial concentration increase, the absolute value of the free energy decreases; therefore, lower temperatures and lower initial concentrations are favorable for the removal of Pb(II) by kaolinite. The Gibbs free energies are all in the range of –20 to 0 kJ/mol, indicating that physical adsorption is the primary adsorption mechanism. As the initial Pb(II) concentration increases, the enthalpy change in adsorption decreases and becomes negative, indicating that the adsorption of Pb(II) onto kaolinite is an exothermic process. The absolute values of the enthalpy change are all less than 40 kJ/mol, further confirming physical adsorption as the primary adsorption mechanism. At different initial concentrations, the entropy change in adsorption is negative, indicating that the entropy of the soil-water interface decreases during the adsorption process [45]. Ionic exchange between Pb^{2+} in solution and the hydrogen atoms of hydroxyls on the surface of soil particles is not the primary adsorption mechanism. One Pb^{2+} ion can equally replace two H^+ ions on hydroxyl groups. Therefore, the entropy on the soil-water interface increases, resulting in a positive entropy change if ionic exchange is the primary mechanism. For bentonite, as the initial concentration of Pb(II) increases from 50 to 200 mg/L, the enthalpy changes in adsorption range from 26.77 to 99.52 kJ/mol, which indicates that adsorption is an endothermic process. The entropy change in adsorption is positive, indicating that the entropy on the soil-water interface increases during the adsorption process. The Gibbs free energy is in the range of –30.63 to –40.62 kJ/mol, indicating that the adsorption reaction is a spontaneous process [34]. The free energy decreases as the temperature increases, indicating that the removal of Pb(II) by bentonite is easier at higher temperatures [46].

3.6. Regeneration of kaolinite and bentonite

Desorption and regeneration are important factors for potential application in real wastewater treatment [19,24]. In this study, 0.10 M HCl was used as the desorption reagent,

and five cycles of adsorption -desorption were performed to study the removal performance of Pb(II) by kaolinite and bentonite. The results indicated that after five adsorption–desorption cycles under the optimum condition, the removal rates of Pb(II) onto kaolinite and bentonite declined by 12% and 15%, respectively, suggesting that both kaolinite and bentonite are cost-effective materials with excellent adsorption capability and easy regeneration properties for the treatment of Pb(II)-containing wastewater [19,24].

3.7. Comparison of the adsorption capacities of clay adsorbents

To compare the adsorption characteristics of Pb(II) onto clays, Table 5 lists the maximum adsorption capacity of Pb(II) on various clay adsorbents. The adsorption capacity of Dalian kaolinite reaches 18.86 mg/g, which is significantly higher than that of Fujian kaolinite [33], Iran kaolinite [30], and Egypt kaolinite [54]. In addition, the adsorption capacity of Algerian kaolinite [35] is superior to that of Dalian kaolinite. For Heishan bentonite, the adsorption capacity reached 27.23 mg/g, which is higher than those of Egyptian Na-bentonite [43], Fujian fly ash/Liaoning Ca-bentonite [55], South Africa Na-bentonite/carbon black [56], and Iran bentonite [57]. Therefore, natural Dalian kaolinite and Heishan bentonite without modification showed an excellent adsorption capacity for Pb(II), suggesting that they are suitable for Pb(II) removal from wastewater in practical engineering.

4. Conclusions

The adsorption characteristics of natural kaolinite and bentonite clays towards Pb(II) were assessed, and the effects of parameters such as the solid-to-liquid ratio, pH, temperature, and reaction time on the adsorption performance of Pb(II) were evaluated. For kaolinite, as the solid-to-liquid ratio increases, the adsorption capacity decreases. The pH of the solution has a significant effect on Pb(II) removal, and the best pH range is 2.91 to 6.0. For bentonite, as the

Table 5
Comparison of maximum adsorption capacities of Pb(II) onto clay adsorbents

Adsorbent	pH	T (°C)	r (g/L)	C_0 (mg/L)	q_m (mg/g)	References
Moroccan clays	4.5	25	15	10–200	2.45	[22]
Ukrainian chamotte clay	6.0	–	10	5–500	11.06	[20]
India natural clay	7.0	30	10	10–20	25.07	[28]
Algerian kaolinite	7.0	25	4	50–150	57.30	[35]
Fujian kaolinite	7.0	30	25	10–150	2.35	[33]
Nigeria kaolinite	5.5	40	10	60–400	19.96	[32]
Iran kaolinite	4.5	20	100	50	7.75	[30]
Egypt kaolinite	6.0	25	1	5–250	15.52	[54]
Egyptian Na-bentonite	3.8	25	2.5	10	5.44	[43]
Fujian fly ash/Liaoning Ca-bentonite	6.0	25	10	100	14.88	[55]
South Africa Na-bentonite/carbon black	6	25	2–8	10–25	7.69	[56]
Iran bentonite	3.0	27	10	10–100	8.55	[57]
Turkey bentonite	5	25	12.5	50–800	55.56	[58]
Dalian kaolinite	6.0	20	6.0	20–300	18.86	This study
Heishan bentonite	7.0	40	10.0	50–500	27.23	This study

solid-to-liquid ratio increases, the adsorption capacity initially increases up to a peak value and then decreases. The removal rate is approximately 100% at pH = 8.0–12.0. The adsorption processes of Pb(II) onto both kaolinite and bentonite are rapid adsorption processes, in which adsorption equilibrium is reached within 120 min. The pseudo-second-order kinetic model fits the kinetic experimental values best, and the adsorption mechanisms of kaolinite and bentonite are controlled by both liquid film diffusion and particle internal diffusion. Langmuir model can best simulate the isothermal adsorption of Pb(II) onto clays. The maximum adsorption capacity of kaolinite was 18.86 mg/g at initial concentrations of 20 to 300 mg/L, pH 6.0, dose of 6.0 g/L and 20°C. The maximum adsorption capacity of bentonite was 27.23 mg/g at initial concentration of 50 to 500 mg/L, pH 7.0, dose of 10.0 g/L and 40°C. The adsorption thermodynamics of Pb(II) onto kaolinite is a spontaneous, exothermic, and entropy-decreasing process, whereas adsorption onto bentonite is an endothermic process. Therefore, both natural kaolinite and bentonite were proven to be efficient and effective adsorbents for the removal of Pb(II) from wastewater.

Symbols

b	—	Langmuir model constant, L/mg
c	—	Intercept related to the boundary layer thickness, dimensionless
C_0	—	Initial concentration of heavy metal ions, mg/L
C_e	—	Equilibrium concentration of heavy metal ions, mg/L
E	—	Average adsorption free energy, kJ/mol
h	—	Initial adsorption rate, mg/g/min
k	—	Model constant related to free energy, mol²/kJ²
k_1	—	Adsorption rate constant, 1/min
k_2	—	Adsorption rate constant, g/mg/min
K_D	—	Distribution coefficient at the solid-liquid interface, mL/g
K_F	—	Model constant related to the adsorption capacity, mg/g
k_{int}	—	Internal diffusion rate constant, mg/g/min$^{1/2}$
m	—	Mass of the adsorbent, g
n	—	Model constant related to adsorption strength, dimensionless
Q	—	Single-layer maximum adsorption capacity, mg/g
q_e	—	Adsorption capacity at equilibrium, mg/g
q_t	—	Adsorption capacity at time t, mg/g
R	—	Removal rate, %
r	—	Solid-to-liquid ratio, g/L
R_L	—	Separation factor, dimensionless
T	—	Thermodynamic temperature, K
V	—	Volume of the solution, L
ΔG	—	Gibbs free energy, kJ/mol
ΔH	—	Enthalpy change, kJ/mol
ΔS	—	Entropy change, J/mol/K
ε	—	Polanyi potential, kJ/mol

Author disclosure statement

No competing financial interests exist.

References

[1] T.A. Khan, M. Nazir, E.A. Khan, Magnetically modified multiwalled carbon nanotubes for the adsorption of Bismarck brown R and Cd(II) from aqueous solution: batch and column studies, Desal. Water Treat., 57 (2016) 19374–19390.

[2] T.A. Khan, S.A. Chaudhry, I. Ali, Equilibrium uptake, isotherm and kinetic studies of Cd(II) adsorption onto iron oxide activated red mud from aqueous solution, J. Mol. Liq., 202 (2015) 165–175.

[3] M.F. Siddiqui, E.A. Khan, T.A. Khan, Synthesis of MoO₃/polypyrrole nanocomposite and its adsorptive properties toward cadmium(II) and nile blue from aqueous solution: equilibrium isotherm and kinetics modeling, Environ. Prog. Sustainable Energy, 38 (2019) e13249.

[4] R. Aigbe, D. Kavaz, Unravel the potential of zinc oxide nanoparticle-carbonized sawdust matrix for removal of lead(II) ions from aqueous solution, Chin. J. Chem. Eng., 29 (2021) 92–102.

[5] C. Xiong, C. Xue, L.Y. Huang, P. Hu, P. Fan, S.X. Wang, X.T. Zhou, Z.J. Yang, Y.Q. Wang, H.B. Ji, Enhanced selective removal of Pb(II) by modification low-cost bio-sorbent: Experiment and theoretical calculations, J. Cleaner Prod., 316 (2021) 128372, doi: 10.1016/j.jclepro.2021.128372.

[6] GB 8978-1996, Integrated Water Discharge Standard, 1997.

[7] N.N. Zhang, N. Cheng, Q. Liu, Functionalized biomass carbon-based adsorbent for simultaneous removal of Pb²⁺ and MB in wastewater, Materials, 14 (2021) 3537, doi: 10.3390/ma14133537.

[8] W. Ahmed, S. Mehmood, A. Nunez-Delgado, S. Ali, M. Qaswar, A. Shakoor, M. Mahmood, D.Y. Chen, Enhanced adsorption of aqueous Pb(II) by modified biochar produced through pyrolysis of watermelon seeds, Sci. Total Environ., 784 (2021) 147136, doi: 10.1016/j.scitotenv.2021.147136.

[9] M. Chen, X.F. Wang, H. Zhang, Comparative research on selective adsorption of Pb(II) by biosorbents prepared by two kinds of modifying waste biomass: highly-efficient performance, application and mechanism, J. Environ. Manage., 288 (2021) 112388, doi: 10.1016/j.jenvman.2021.112388.

[10] S. Cheng, Y.Z. Liu, B.L. Xing, X.J. Qin, C.X. Zhang, H.Y. Xia, Lead and cadmium clean removal from wastewater by sustainable biochar derived from poplar saw dust, J. Cleaner Prod., 314 (2021) 128074, doi: 10.1016/j.jclepro.2021.128074.

[11] L. Khalfa, A. Sdiri, M. Bagane, M.L. Cervera, A calcined clay fixed bed adsorption studies for the removal of heavy metals from aqueous solutions, J. Cleaner Prod., 278 (2021) 123935, doi: 10.1016/j.jclepro.2020.123935.

[12] I.V. Joseph, L. Tosheva, G. Miller, A.M. Doyle, Fau-type zeolite synthesis from clays and its use for the simultaneous adsorption of five divalent metals from aqueous solutions, Materials, 14 (2021) 3738, doi: 10.3390/ma14133738.

[13] T.T. Li, X.X. Huang, Q. Wang, G. Yang, Adsorption of metal ions at kaolinite surfaces: ion-specific effects, and impacts of charge source and hydroxide formation, Appl. Clay Sci., 194 (2020) 105706, doi: 10.1016/j.clay.2020.105706.

[14] T.A. Khan, M. Nazir, E.A. Khan, U. Riaz, Multiwalled carbon nanotube-polyurethane (MWCNT/PU) composite adsorbent for Safranin T and Pb(II) removal from aqueous solution: batch and fixed-bed studies, J. Mol. Liq., 212 (2015) 467–479.

[15] S.A. Chaudhry, T.A. Khan, I. Ali, Adsorptive removal of Pb(II) and Zn(II) from water onto manganese oxide-coated sand: isotherm, thermodynamic and kinetic studies, Egypt. J. Basic Appl. Sci., 3 (2016) 287–300.

[16] T.A. Khan, V.V. Singh, Removal of cadmium(II), lead(II), and chromium(VI) ions from aqueous solution using clay, Toxicol. Environ. Chem., 92 (2010) 1435–1446.

[17] T.A. Khan, V. Singh, I. Ali, Sorption of Cd(II), Pb(II), and Cr(VI) metal ions from wastewater using bottom fly ash as a low cost sorbent, J. Environ. Prot. Sci., 3 (2009) 124–132.

[18] T.A. Khan, A.A. Mukhlif, E.A. Khan, D.K. Sharma, Isotherm and kinetics modeling of Pb(II) and Cd(II) adsorptive uptake from aqueous solution by chemically modified green algal biomass, Model. Earth Syst. Environ., 2 (2016) 1–13.

[19] M. Sölener, S. Tunali, A.S. Özcan, A. Özcan, T. Gedikbey, Adsorption characteristics of lead(II) ions onto the clay/poly(methoxyethyl)acrylamide (PMEA) composite from aqueous solutions, Desalination, 223 (2008) 308–322.

[20] A.B. Rakhym, G.A. Seilkhanova, T.S. Kurmanbayeva, Adsorption of lead(II) ions from water solutions with natural zeolite and chamotte clay, Mater. Today, 31 (2020) 482–485.

[21] X.Q. Yin, L. Yu, X.H. Luo, Z. Zhang, H.M. Sun, A.A. Mosa, N. Wang, Sorption of Pb(II) onto <1 μm effective diameter clay minerals extracted from different soils of the Loess Plateau, China, Geoderma, 337 (2019) 1058–1066.

[22] M. Ahrouch, J.M. Gatica, K. Draoui, D. Bellido, H. Vidal, Lead removal from aqueous solution by means of integral natural clays honeycomb monoliths, J. Hazard. Mater., 365 (2019) 519–530.

[23] A. Sdiri, M. Khairy, S. Bouaziz, S. EI-Safty, A natural clayey adsorbent for selective removal of lead from aqueous solutions, Appl. Clay Sci., 126 (2016) 89–97.

[24] D. Humelnicu, M. Ignat, M. Suchea, Evaluation of adsorption capacity of montmorillonite and aluminium-pillared clay for Pb^{2+}, Cu^{2+} and Zn^{2+}, Acta Chim. Slov., 62 (2015) 947–957.

[25] N.D. Mu'azu, Evaluation of the influence of clay montmorillonite content on the aqueous uptake of lead and zinc, Water Environ. Res., 90 (2018) 771–782.

[26] M. EI. Batouti, F.M. Abouzeid, Pb(II) adsorption from aqueous solution using modified sodium montmorillonite clay: equilibrium and kinetic study, Rev. Roum. Chim., 61 (2016) 5–13.

[27] M. Abdelwaheb, K. Jebali, H. Dhaouadi, S. Dridi-Dhaouadi, Adsorption of nitrate, phosphate, nickel and lead on soils: risk of groundwater contamination, Ecotoxicol. Environ. Saf., 179 (2019) 182–187.

[28] A. Kushwaha, R. Rani, J.K. Patra, Adsorption kinetics and molecular interactions of lead [Pb(II)] with natural clay and humic acid, Int. J. Environ. Sci. Technol., 17 (2020) 1325–1336.

[29] EI. Unuabonah, K.O. Adebowale, A.E. Ofomaja, Two-stage batch adsorber design: a time-dependent Langmuir model for adsorption of Pb^{2+} and Cd^{2+} onto modified kaolinite clay, Water Air Soil Pollut., 200 (2009) 133–145.

[30] S. Shahmohammadi-Kalalagh, H. Babazadeh, A.H. Nazemi, M. Manshouri, Isotherm and kinetic studies on adsorption of Pb, Zn and Cu by kaolinite, Caspian J. Environ. Sci., 9 (2011) 243–255.

[31] I. Fatimah, Preparation, characterization and physicochemical study of 3-amino propyl trimethoxy silane-modified kaolinite for Pb(II) adsorption, J. King Saud Univ. Sci., 30 (2018) 250–257.

[32] EI. Unuabonah, K.O. Adebowale, B.I. Olu-Owolabi, L.Z. Yang, L.X. Kong, Adsorption of Pb(II) and Cd(II) from aqueous solutions onto sodium tetraborate-modified kaolinite clay: equilibrium and thermodynamic studies, Hydrometallurgy, 93 (2008) 1–9.

[33] M.Q. Jiang, X.Y. Jin, X.Q. Lu, Z.L. Chen, Adsorption of Pb(II), Cd(II), Ni(II) and Cu(II) onto natural kaolinite clay, Desalination, 252 (2010) 33–39.

[34] I.M. EI-Naggar, S.A. Ahmed, N. Shehata, E.S. Sheneshen, M. Fathy, A. Shehata, A novel approach for the removal of lead(II) ion from wastewater using kaolinite/smectite natural composite adsorbent, Appl. Water Sci., 9 (2019) 1–13.

[35] S. Bahah, S. Nacef, D. Chebli, A. Bouguettoucha, B. Djellouli, A new highly efficient Algerian clay for the removal of heavy metals of Cu(II) and Pb(II) from aqueous solutions: characterization, fractal, kinetics, and isotherm analysis, Arabian J. Sci. Eng., 45 (2020) 205–218.

[36] D.A. Glatstein, F.M. Francisca, Influence of pH and ionic strength on Cd, Cu and Pb removal from water by adsorption in Na-bentonite, Appl. Clay Sci., 118 (2015) 61–67.

[37] J.G. Meneguin, M.P. Moises, T. Karchiyappan, S.H.B. Faria, M.L. Gimenes, M.A.S.D. de Barros, S. Venkatachalam, Preparation and characterization of calcium treated bentonite clay and its application for the removal of lead and cadmium ions: adsorption and thermodynamic modeling, Process Saf. Environ. Prot., 111 (2017) 244–252.

[38] J.A. Alexander, M.A.A. Zaini, A. Surajudeen, E.N.U. Aliyu, A.U. Omeiza, Insight into kinetics and thermodynamics properties of multicomponent lead(II), cadmium(II) and manganese(II) adsorption onto Dijah-Monkin bentonite clay, Part. Sci. Technol., 36 (2018) 569–577.

[39] J.A. Alexander, M.A.A. Zaini, S. Abdulsalam, U.A. EI-Nafaty, U.O. Aroke, Isotherm studies of lead(II), manganese(II), and cadmium(II) adsorption by Nigerian bentonite clay in single and multimetal solutions, Part. Sci. Technol., 37 (2019) 399–409.

[40] L. Perelomov, B. Sarkar, M.M. Rahman, A. Goryacheva, R. Naidu, Uptake of lead by Na-exchanged and Al-pillared bentonite in the presence of organic acids with different functional groups, Appl. Clay Sci., 119 (2016) 417–423.

[41] V.J. Inglezakis, M.A. Stylianou, D. Gkantzou, M.D. Loizidou, Removal of Pb(II) from aqueous solutions by using clinoptilolite and bentonite as adsorbents, Desalination, 210 (2007) 248–256.

[42] C.L. Zou, W. Jiang, J.Y. Liang, X.H. Sun, Y.Y. Guan, Removal of Pb(II) from aqueous solutions by adsorption on magnetic bentonite, Environ. Sci. Pollut. Res., 26 (2019) 1315–1322.

[43] A.A. Taha, M.A. Shreadah, A.M. Ahmed, H.F. Heiba, Multi-component adsorption of Pb(II), Cd(II), and Ni(II) onto Egyptian Na-activated bentonite; equilibrium, kinetics, thermodynamics, and application for seawater desalination, J. Environ. Chem. Eng., 4 (2016) 1166–1180.

[44] W. Mo, Q.Z. He, X.J. Su, S.J. Ma, J.P. Feng, Z.L. He, Preparation and characterization of a granular bentonite composite adsorbent and its application for Pb^{2+} adsorption, Appl. Clay Sci., 159 (2018) 68–73.

[45] S.M. Awadh, F.H. Abdulla, Purification of aqueous solutions from Pb(II) by natural bentonite: an empirical study on chemical adsorption, Environ. Earth Sci., 76 (2017) 386, doi: 10.1007/s12665-017-6725-3.

[46] B.H. Graimed, Z.T.A. Ali, Thermodynamic and kinetic study of the adsorption of Pb(II) from aqueous solution using bentonite and activated carbon, Al-Khwarizmi Eng. J., 9 (2013) 48–56.

[47] T.A. Khan, S. Dahiya, I. Ali, Use of kaolinite as adsorbent: equilibrium, dynamics and thermodynamic studies on the adsorption of Rhodamine B from aqueous solution, Appl. Clay Sci., 69 (2012) 58–66.

[48] K.G. Bhattacharyya, S.S. Gupta, Adsorption of a few heavy metals on natural and modified kaolinite and montmorillonite: a review, Adv. Colloid Interface Sci., 140 (2008) 114–131.

[49] S.A. Khan, M.F. Siddiqui, T.A. Khan, Ultrasonic-assisted synthesis of polyacrylamide/bentonite hydrogel nanocomposite for the sequestration of lead and cadmium from aqueous phase: equilibrium, kinetics and thermodynamic studies, Ultrason. Sonochem., 60 (2020) 104761.

[50] Y. Wang, X.W. Tang, H.Y. Wang, W. Liu, Sorption and desorption behaviors of heavy metal Mn(II) on loess soil, Chin. J. Geotech. Eng., 33 (2011) 369–373.

[51] D.L. Zhao, G.D. Sheng, J. Hu, C.L. Chen, X.K. Wang, The adsorption of Pb(II) on Mg_2Al layered double hydroxide, Chem. Eng. J., 171 (2011) 167–174.

[52] A.E. Ofomaja, E.B. Naidoo, Biosorption of lead(II) onto pine cone powder: studies on biosorption performance and process design to minimize biosorbent mass, Carbohydr. Polym., 82 (2010) 1031–1042.

[53] V. Srivastava, C.H. Weng, V.K. Singh, Y.C. Sharma, Adsorption of nickel ions from aqueous solutions by nano alumina: kinetic, mass transfer, and equilibrium studies, J. Chem. Eng. Data, 56 (2011) 1414–1422.

[54] A. Maged, I.S. Ismael, S. Kharbish, B. Sarkar, S. Peraniemi, A. Bhatnagar, Enhanced interlayer trapping of Pb(II) ions within kaolinite layers: intercalation, characterization, and sorption studies, Environ. Sci. Pollut. Res. Int., 27 (2019) 1870–1887.

[55] N. Xie, J.Y. Zhang, P.D. Liu, Preparation of fly ash/bentonite particles and adsorption experiment of Pb^{2+}, Acta Miner. Sin., 40 (2020) 41–46.

[56] H. Chiririwa, T. Matthews, B. Nyoni, S. Majoni, B. Naidoo, Adsorption of lead and copper by carbon black and sodium bentonite composite material: a study on adsorption isotherms and kinetics, Asian J. Chem., 29 (2017) 2761–2766.

[57] A. Esmaeili, H. Eslami, Efficient removal of Pb(II) and Zn(II) ions from aqueous solutions by adsorption onto a native natural bentonite, MethodsX, 6 (2019) 1979–1985.

[58] N. Baylan, A.E. Mericboyu, Adsorption of lead and copper on bentonite and grapeseed activated carbon in single- and binary-ion systems, Sep. Sci. Technol., 51 (2016) 2360–2368.